

Visualizing priming of virus-specific CD8⁺ T cells by infected dendritic cells *in vivo*

Christopher C. Norbury*, Daniela Malide, James S. Gibbs, Jack R. Bennink and Jonathan W. Yewdell

Published online: 4 February 2002, DOI: 10.1038/ni762

The rational design of vaccines that elicit CD8⁺ T cell responses requires knowledge of the identity of the antigen-presenting cell (APC), the location and time of presentation and the nature of the antigen presented by the APC. Here we address these questions for an antigen encoded by a recombinant vaccinia virus. We found that, following local infection, vaccinia virus infected macrophages and dendritic cells in draining lymph nodes. However, only the dendritic cells presented antigen to naïve CD8⁺ T cells, as determined by direct visualization of sectioned nodes by confocal microscopy. Presentation occurred as rapidly as 6 h after inoculation and quickly declined in parallel with the number of infected cells present in the nodes. These data provide direct evidence that virus-infected APCs prime naïve CD8⁺ T cells *in vivo*.

CD8⁺ T cells recognize peptides of 8–11 amino acids in length that are displayed by major histocompatibility complex (MHC) class I molecules expressed at the surface of antigen-presenting cells (APCs). Studies of antigen presentation *in vitro* have provided a basic outline for how cells generate MHC class I peptide ligands from polypeptides that are biosynthesized by APCs^{1,2} and—at a more rudimentary level—from polypeptides acquired by APCs from other cells³. This knowledge should eventually facilitate the rational design of vaccines that optimally elicit CD8⁺ T cells responses. There is great interest in developing such vaccines to prevent or treat a number of infectious diseases and malignancies.

To apply this knowledge to vaccine design, a number of fundamental questions must be answered regarding the presentation of antigens to naïve CD8⁺ T cells *in vivo*. Which cells present antigen? Where and when does presentation occur? What form of antigen is presented? How do the answers to these questions vary with the nature of the immunogen and the route of immunization?

We addressed here the first three of these questions by analyzing CD8⁺ T cell response to a well defined antigen expressed by a recombinant vaccinia virus (rVV), a vector that is a mainstay of current vaccine trials. Despite the fact that billions of individuals were immunized with infectious VV during the smallpox eradication campaign, little is known about how VV-encoded proteins are presented to the immune system.

Results

Strategy

The most definitive method for localizing antigen presentation *in vivo* is to directly visualize the interaction of APCs with T cells. This has only been reported for CD4⁺ T cells, and then only in a few systems⁴. In these studies, the presentation of antigens in APCs was inferred based on the antigen-dependent interaction of CD4⁺ T cells with APCs. When studying endogenous antigen presentation to CD8⁺ T cells, infected APCs can be

visualized by detecting the expression of virus-encoded antigens targeted to organelles that are poorly accessed by exogenous proteins, such as the nucleus. To enable visualization of virus-infected cells in both live and fixed tissues, we generated a rVV that expressed a chimeric protein consisting of influenza virus nucleoprotein genetically appended to the NH₂-terminus of enhanced green fluorescent protein (EGFP). Due to the karyophilic properties of the NP, the chimeric protein strongly localized to the nuclei of infected cells; consequently, the presence of nuclear NP-EGFP indicated that the protein was synthesized by the cell.

Due to the low frequency and clonal heterogeneity of virus-specific CD8⁺ T cells, visualizing responding naïve virus-specific CD8⁺ T cells is difficult, if not impossible, with the available technology. We therefore used naïve T cells from T cell receptor (TCR)-transgenic mice. To make the findings more general, two TCR-transgenics were used: OT-I—which possess CD8⁺ T cells specific for the ovalbumin (OVA) peptide SIINFEKL in association with H-2K^b—and F5—which possess CD8⁺ T cells specific for the influenza NP60 NP peptide ASNENMDAM in association with H-2D^b. We inserted SIINFEKL in the chimeric NP-EGFP protein at the NP and EGFP junction to create an rVV that expressed NP-SIINFEKL-EGFP, referred to hereafter as VV.NP-S-EGFP.

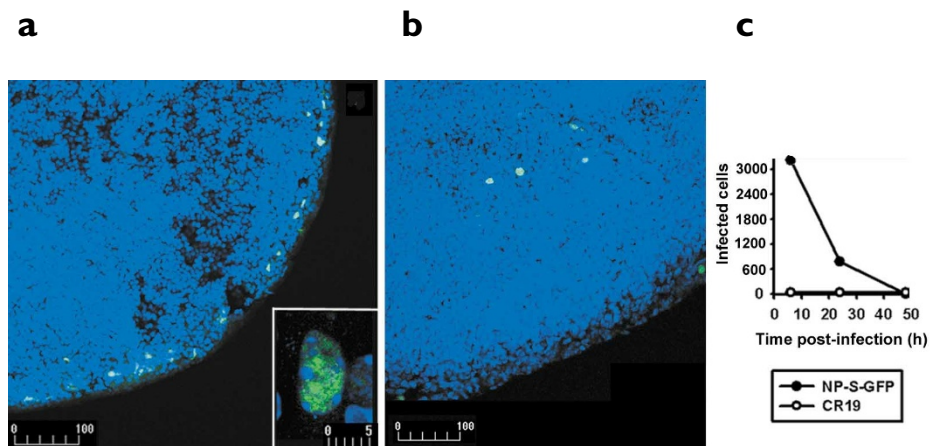
Localization of virus-infected cells in lymph nodes

We infected C57BL/6 (B6) mice in their footpads with 10⁷ plaque-forming units (PFU) of VV.NP-S-EGFP and removed the draining popliteal lymph nodes (PLNs) 6 h later. Nodes were frozen, sectioned and stained with TO-PRO-3 iodide, a fluorescent DNA stain that identifies cellular nuclei. As determined by EGFP direct fluorescence, we found that the distribution of infected cells was largely limited to the PLN periphery, which borders the subcapsular sinus (Fig. 1a). All detectable EGFP fluorescence colocalized with TO-PRO-3 iodide staining; this indicated that NP was present in the nucleus and, therefore, that the EGFP⁺ cells were

Laboratory of Viral Diseases, National Institute of Allergy and Infectious Diseases, National Institutes of Health, Bethesda, MD 20892-0440, USA. *Present address: Department of Microbiology and Immunology, Pennsylvania State University College of Medicine, Hershey, PA 17033, USA.

Correspondence should be addressed to J.Y. (jyewdell@nih.gov).

Figure 1. Infection of lymph node cells with VV after footpad infection. Draining PLNs were removed (a) 6 h or (b) 24 h after footpad injection, frozen, sectioned, fixed and stained with the DNA-binding dye TO-PRO-3 iodide in order to identify the nuclei. Inset in a shows, at high magnification, NP-S-EGFP (green) overlapping with TO-PRO-3 iodide nuclear staining (blue). All green fluorescence shown was above the background amounts observed in nodes from uninfected mice or mice infected with a control non-EGFP-expressing rVV. Bars are in μm . (c) PLNs were removed from mice infected with either VVNP-S-EGFP or a control virus (CR19) 6, 24 or 48 h after infection. Cells recovered from homogenized nodes were analyzed for green fluorescence by flow cytometry. The numbers of EGFP⁺ cells were quantified by analyzing equal numbers of cells then adjusting for the number of cells recovered from the nodes at each timepoint. Data are representative of at least three independent experiments.



rVV-infected. We found that the number of EGFP-expressing cells declined sharply during the 6–24 h after virus inoculation (Fig. 1b), and only a few cells were detected by 48 h after inoculation. To accurately quantify this decline, we generated single cell suspensions from PLNs and identified the EGFP-expressing cells by flow cytometry. The number of EGFP⁺ cells was calculated by taking into account the increased number of cells induced by VV-infection (a sixfold increase over the 48 h of infection). This showed an 80% reduction in the absolute number of infected cells between 6 and 24 h, and a further large decrease over the next day to below the limit of detection (Fig. 1c). We estimated that the draining PLNs had ~3000 infected cells at 6 h after inoculation, 600 cells at 24 h and <100 cells at 48 h.

Characterization of VV-infected PLN cells

We next determined which type of PLN cells were infected by staining sections with antibodies that were specific for marker proteins. Based on the subcapsular location, we expected that the majority of infected cells would be macrophages, which are prevalent in this area. Indeed, the majority of infected cells present at 6 h (Fig. 2) and 24 h (data not shown) after infection stained with a monoclonal antibody (mAb) specific for CD169, a macrophage marker. The highly magnified image shows NP-S-EGFP in the nucleus surrounded by cell surface staining of the macrophage with anti-CD169 (Fig. 2b). Staining of sections with mAbs for other macrophage-specific markers—MOMA-1, MOMA-2, F4/80 and anti-CD11b—confirmed that 60–90% of infected cells were typical macrophages (Fig. 2c–f).

We found no evidence for VV infection of neutrophils, B cells or T cells (data not shown). Approximately 10–15% of the infected cells strongly stained with an MHC class II-specific mAb (Fig. 3a) or the DC marker mAb MIDC-8 (Fig. 3b). The morphology of these infected cells was consistent with that of DCs. Together, these findings indicate that nearly all the infected cells we detected in the nodes were macrophages and the remainder were DCs. Similar results were obtained when spleens were sectioned after intravenous (i.v.) viral inoculation (data not shown).

Antigen presentation by node cells *in vitro*

To correlate these findings with antigen presentation, we assessed the capacity of dissociated PLN cells to activate B3Z cells. B3Z is a CD8⁺ T cell hybridoma specific for SIINFEKL–H-2K^b that expresses β -gal under the control of the interleukin 2 (IL-2) promoter, enabling rapid (overnight) histochemical enumeration of activated cells⁵. This is probably the most sensitive method for detecting low frequencies of APCs. In addition, the use of a hybridoma allows enumeration of antigen presentation by infected cells without the potential for cross-presentation by professional APCs. Such APCs may copurify with responding naïve or secondary CD8⁺ T cells, despite extensive efforts to remove these cells. We further maximized the sensitivity of the system by injecting mice with an rVV that expressed SIINFEKL as a cytosolic minigene product. APCs infected with this virus *in vitro* typically express ~20-fold more OVA(257–264)–H-2K^b complexes on their cell surfaces than cells expressing NP-SIINFEKL-EGFP (or full-length OVA) (C. C. N. *et al.*, unpublished data).

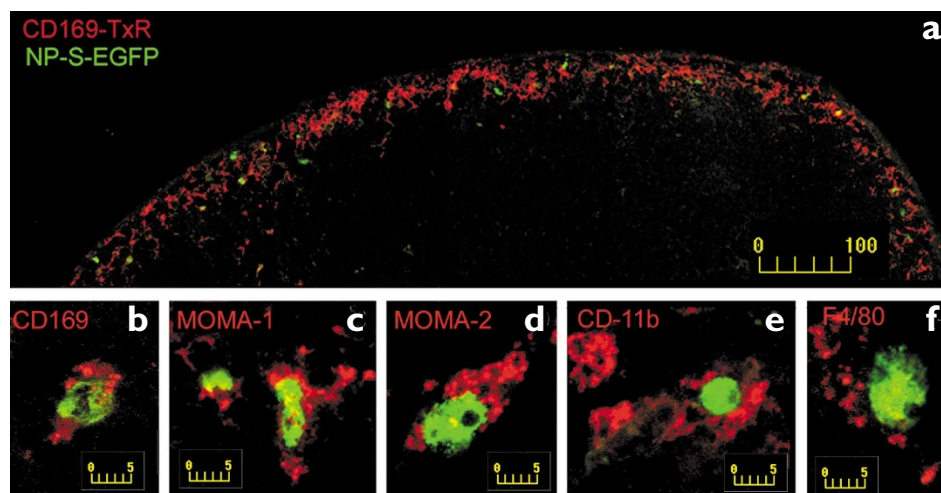


Figure 2. Phenotype of VV-infected PLN cells. Draining PLNs were prepared as in Fig. 1a, and fixed sections were stained with antibodies to macrophages. Anti-CD169 staining (sialoadhesin) is in red; NP-S-EGFP is in green. (a) A montage of sections stained with anti-CD169. (b–f) High-magnification images of cells stained with the indicated antibodies. Bars are in μm ; data are representative of three independent experiments.

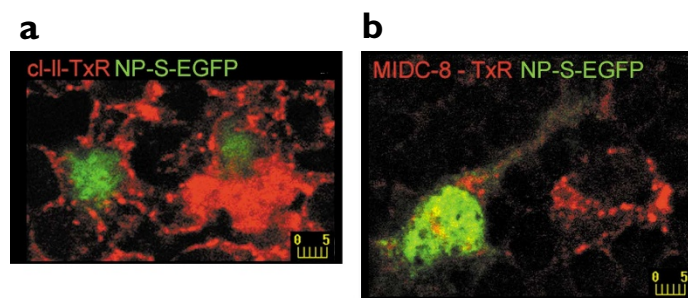


Figure 3. VV infection of PLN DCs. Draining PLNs were prepared as in Fig. 1a and fixed sections were stained with either (a) monoclonal anti-MHC class II or (b) anti-DC (MIDC-8). Bars are in μm ; data are representative of three independent experiments.

Infection of mice with a control virus that did not express SIINFEKL (called CR19) did not activate B3Z cells above the background amounts observed after incubation with PLN cells from uninfected mice. In contrast, B3Z cells were activated by PLN cells derived from mice infected with VV that expressed SIINFEKL. Antigen presentation was maximal at the initial timepoint (6 h after infection) and declined to near background amounts over the next 42 h (Fig. 4a).

We found that the decline in antigen presentation was not accompanied by a concurrent appearance of SIINFEKL-specific lytic activity, which was undetectable at 48 h (Fig. 4b). However, we easily detected lytic activity in PLN cells 5 days after infection. Even after the adoptive transfer of F5 TCR-transgenic CD8^+ T cells to increase the precursor frequency of specific T cells, we could not detect antigen-specific effector function, interferon- γ (IFN- γ) secretion, in the draining lymph node before 3 days after infection (data not shown). This showed that there is a delay between antigen presentation and the acquisition of detectable effector function *in vivo*.

Localization of antigen presentation *in vivo*

We next used transgenic CD8^+ T cells to localize CD8^+ T cell-APC interactions *in vivo*. Purified SIINFEKL-specific T cells from OT-I mice were labeled with a fluorescent red cell tracker (CMTMR) and introduced into B6 mice by i.v. injection. The next day, mice were injected in their footpads with VV.NP-S-EGFP. Six hours after infection, the draining PLNs were removed, thick (25- μm) cryosections were prepared and SIINFEKL-specific T cells and virus-infected cells were visualized by confocal microscopy (Fig. 5). We scanned 25 individual fields with surface areas of 350 μm^2 each using a $\times 20$ objective and setting the confocal pinhole to enable visualization of the entire 25- μm thickness of the section. Individual fields were digitally assembled to reconstitute approximately two-thirds of the entire cryosection (Fig. 5a shows a portion of the composite image that

represents about one-quarter of the node cross-section). Each potential CD8^+ T cell-APC cluster detected was examined in detail by collecting a z-series throughout the region with a $\times 63$ objective and analyzing the interaction of cells using three-dimensional (3D) visualization software. For the purposes of illustration, 2D projections of the 3D datasets are shown in the insets (Fig. 5b-d).

We could easily identify labeled SIINFEKL-specific CD8^+ T cells within the T cell areas of the PLNs, including a minority that were clustered around NP-S-EGFP-expressing cells. Clusters consisted of 2–14 antigen-specific CD8^+ T cells (Fig. 5b-d). Only a small fraction of the infected cells were involved in the clusters. Indeed, nearly all the clusters were located in the node parenchyma, which was up to 200 μm from the periphery. We also observed clustering of antigen-specific CD8^+ T cells around NP-S-EGFP-infected cells in the parenchyma of live nodes visualized by multiphoton and confocal microscopy (Fig. 6a,b, respectively). This showed that it was not an artifact of specimen preparation. The SIINFEKL-specific CD8^+ T cells were able to access the subcapsular sinus, where most of the infected macrophages resided (Fig. 5d). By 24 h after infection—when the number of infected cells had markedly decreased—specific CD8^+ T cells had dispersed to the medullary regions of the node (data not shown).

We repeated this experiment using F5-transgenic CD8^+ T cells and quantified cluster formation in PLNs from mice infected with an rVV that expressed either NP-S-EGFP (Fig. 5g) or NP-S-EGFP with two amino acid substitutions in the NP(366–374) determinant (Fig. 5h). These substitutions abrogated recognition by F5 CD8^+ T cells without altering peptide binding to H-2^b. Counting clusters on ten cryosections (25- μm thick) from each PLN by confocal microscopy, we observed 20 clusters per mm^3 of node; this represented ~ 80 clusters for a single PLN. In contrast, after infection with the nonantigenic rVV with the two amino-acid substitution in NP(366–374) nodes cluster formation averaged 0.1 clusters per mm^3 , despite a similar distribution of infected EGFP⁺ cells. This observation showed that clustering was antigen-specific and not merely a chance encounter of antigen-specific CD8^+ T cells and infected APCs within the T cell areas of the lymph node.

T cells from both the OT-1 and F5 mice formed clusters in the absence of an EGFP-expressing cell. In addition, the clustering of F5 cells around EGFP⁺ cells was ablated following infection with the rVV expressing the 2-amino acid substitutions in the NP(366–374) determinant. This indicated that these clusters were also antigen-specific and could mean either that APCs in these clusters expressed small amounts of endogenous NP-S-EGFP or that the APCs were presenting exogenous NP-S-EGFP acquired from other infected cells (that is, by cross-priming).

We attempted to determine the identity of the cluster-inducing APCs. None of these APCs stained with anti-CD169 (Fig. 5f), which showed that the macrophages were unlikely to activate the naive CD8^+ T cells. In contrast, many of these APCs stained with the DC-specific mAb

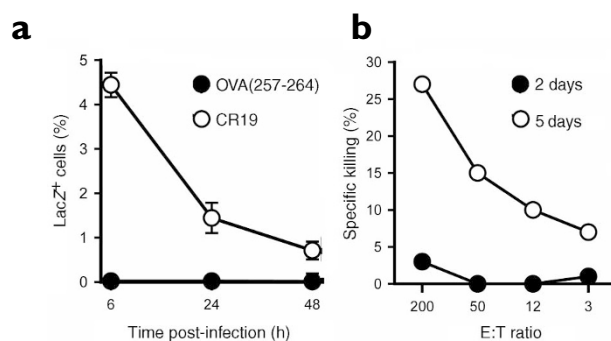


Figure 4. Time-course of antigen presentation in PLNs. (a) Mice were infected in the footpads with either a VV expressing the OVA(257–264) determinant or a control VV (CR19). Single cell suspensions derived from draining PLNs were incubated overnight with the OVA(257–264)-specific LacZ b3Z hybridoma cells. The percentage of activated cells was determined by expression of β -galactosidase, as measured visually by counting blue cells after incubation with X-gal. (b) Mice were infected in their footpads with a VV expressing the OVA(257–264) determinant. Single-cell suspensions derived from draining PLNs 2 or 5 days after infection were incubated at various effector to target (E:T) ratios with ^{51}Cr -labeled EL4 cells that had been pulsed with OVA(257–264) or VSV NP(52–59) peptide for 4 h. Lysis of the target cells was recorded. Results are shown after the background lysis values of VSV NP(52–59)-pulsed cells had been subtracted. Data are representative of at least three independent experiments.

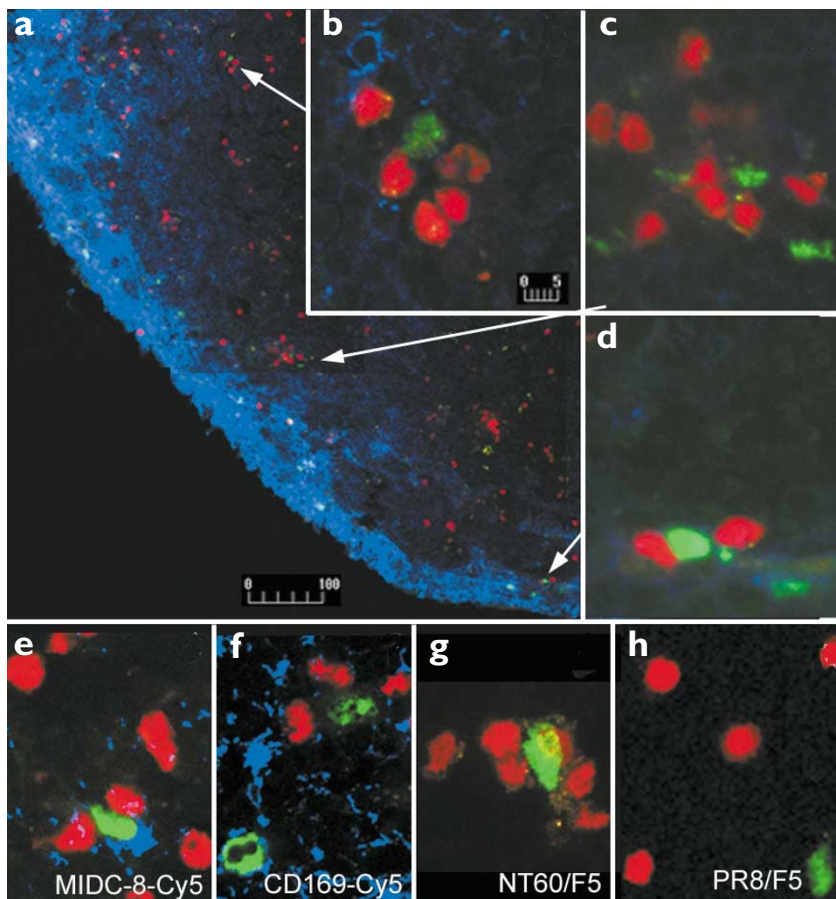


Figure 5. Clustering of naïve T cells around infected DCs. CD8⁺ T cells purified from OT-I (a–f) or F5 (g,h) TCR-transgenic mice, labeled with red cell tracker (CM-TMR) were injected into mice. Mice were infected with either NP-S-EGFP containing either the NT60 NP sequence at aa 366–374 (ASNENMDAM) (a–d) or the PR8 NP sequence (ASNENMETM) (h). Six hours later the PLNs were collected and the relative locations of the transferred (red) and EGFP-expressing cells were examined. (b–d) Magnified views of the regions indicated by arrows, which show clusters of T cells around infected cells. EGFP-expressing cell in the middle of a cluster binds a DC-specific mAb (e, antibody staining is shown in blue), but not a macrophage-specific mAb (f), which stains other EGFP⁺ cells in the section. Note the positive staining of CD169⁺ cells, which are not part of a cluster in f. Bars are in μm ; data are representative of at least three independent experiments.

the node. Therefore, it was not possible to visualize acquisition of effector function and antigen presentation.

Priming of naïve T cells by infected DCs

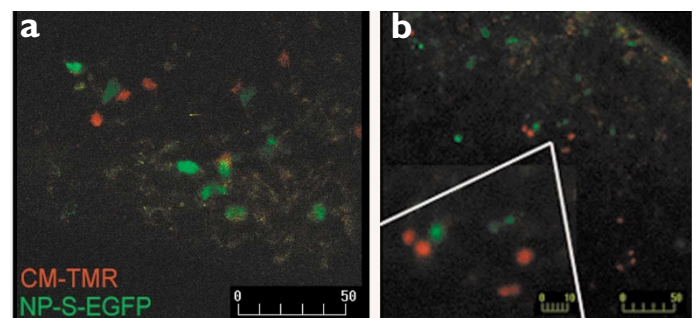
To confirm that infected DCs are capable of activating naïve CD8⁺ T cells *in vivo*, we infected freshly isolated splenocytes *in vitro* with an rVV—VV.NT60 NP(366–374)—that expressed the influenza NT60 determinant as a cytosolic minigene product. We then tested their capacity to activate F5-transgenic CD8⁺ T cells that had been adoptively transferred into mice. Flow cytometric analysis of infected splenocytes after staining with marker mAbs showed the infection of 20–30% of splenocytes that encompassed a wide variety of cell types: these included DCs, macrophages, B cells and some T cells (data not shown). To eliminate complications due to the potential transfer of infectious VV to recipient mice and re-presentation of NP(366–374) by recipient APCs, we transferred splenocytes into mice that were deficient in one of the transporter of antigen processing subunits, TAP1. NP(366–374) is not presented to F5 cells that have been adoptively transferred into TAP^{-/-} mice after direct infection of mice with VV.NT60 NP(366–374)⁷ or by injection of MHC-mismatched cells infected with rVV that expressed either the minigene product or full-length NP (C. C. N. *et al.*, unpublished data). Therefore, neither direct presentation by virus-infected recipient cells nor recipient cell cross-presentation of antigen derived from infected cells can account for T cell activation in this system.

Sixteen hours after the transfer of F5-transgenic CD8⁺ T cells and VV.NT60 NP(366–374)-infected splenocytes into TAP^{-/-} mice, there was a marked activation of F5 cells recovered from spleens. This was indicated by an increase in the percentage of F5 cells with amplified cell surface expression of CD69 or CD25 (also known as IL-2 receptor)

MIDC-8 (Fig. 5e). We were unable to determine whether the APCs that did not stain with MIDC-8 did not express the DC marker or whether the thicker sections required to identify the clusters (25 μm versus 8 μm for optimal cell staining) prevented staining with the MIDC-8 mAb because the cytosol of the cells was inaccessible. Antigen-specific clustering of CD8⁺ T cells around infected DCs, but not infected macrophages, was also observed in the spleen after *i.v.* infection (data not shown).

The DC-centered clusters that we observed in the PLNs and spleen were similar to those observed in studies of the activation of naïve CD4⁺ T cells⁶; they likely represented interactions that result in the priming of naïve CD8⁺ T cells by DCs. However, specific induction of effector mechanisms or proliferation of naïve TCR-transgenic CD8⁺ T cells required a minimum of 24 h. At this timepoint, antigen presentation in the node had declined sharply (Fig. 4) and infected cells could no longer be observed in

Figure 6. Interactions between CD8⁺ T cells and infected cells visualized in a living lymph node. Freshly excised nodes from Fig. 5 were immobilized in a drop of 1.8% agarose, covered with red phenol-free Dulbecco's modified Eagle's medium supplemented with 20 mM HEPES and 1 g/l of glucose (pH 7.4); the dish was then placed in a temperature controller. (a) A multiphoton or (b) standard confocal microscope was used to image the intact node (see Methods). (a) Image is a projection of a z-series spanning a depth of 25 μm into the tissue with a z-axis step-size of 5 μm (from a depth of ~250 μm into the node). (b) Image is a single optical section of a confocal image from a depth of ~80 μm into the node; the inset is a magnified view of the region just above it. Bars are in μm ; data represent two of three independent experiments.



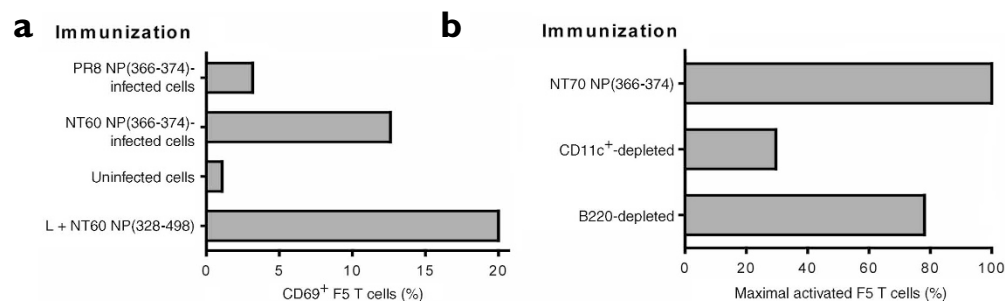


Figure 7. Priming of naïve T cells by infected APCs. TAP1^{-/-} mice were irradiated and purified T cells from F5 TCR-transgenic mice were transferred. (a) Mice were immunized with spleen cells from normal mice infected with VV expressing either NT60 NP(366–374) or PR8 NP(366–374). Sixteen hours later, spleens were removed and the percentage of F5 (CD8⁺Vβ11⁺) cells that showed up-regulation of CD69 were scored. (b) Splenic APCs were depleted of either B cells (B220⁺) or DCs (CD11c⁺) before transfer. Data are a percentage of the maximal signal obtained after transfer of NT60 NP(366–374)-infected splenocytes and are representative of two to four independent experiments.

(Fig. 7a and data not shown) and decreased cell surface expression of CD62L (also known as L-selectin) (data not shown). This showed that transferred splenocytes can activate naïve CD8⁺ T cells in the absence of cross-priming in recipient mice. Activation was specific for the NP(366–374) determinant because, compared to those in uninfected mice, F5 T cells recovered from mice infected with VV.PR8 NP(366–374), a negative control VV which expressed a nonantigenic form of the cytosolic minigene product showed no changes in activation marker expression. The amount of activation was ~50% of that observed when mice were infected with L+ NP(328–498), a positive control rVV that expressed an endoplasmic reticulum-targeted fragment NP that is presented in a TAP-independent manner^{7,8}.

To establish whether infected DCs in the splenic APC population induced the activation of naïve F5 CD8⁺ T cells *in vivo*, we depleted DCs from the transferred VV-infected population using magnetic beads coated with a CD11c-specific mAb (Fig. 7b). This markedly reduced F5 CD8⁺ T cell activation, whereas cell depletion with an mAb specific for B220—which is expressed on a large proportion of infected spleen cells—had only a minor effect on activation. Consistent with these results, a partially purified preparation of splenic (but not bone marrow-derived) DCs infected with VV.NT60 NP(366–374) activated F5 CD8⁺ T cells (data not shown).

Discussion

The nature of APCs and the antigens that they present to naïve CD8⁺ T cells that are responding to viral infections is currently a much-debated issue. Some believe that, with few exceptions, professional APCs cross-present exogenous antigens. Others espouse the view that, with equally few exceptions, endogenous antigens are presented by both professional and nonprofessional APCs. It is likely that the truth lies somewhere in between these extreme views and is likely to vary according to the infectious agent studied.

Analyzing antigen presentation *in vivo* is a challenging exercise, and the approaches used to date have largely been indirect. Several groups have identified APCs from virus-infected mice that activate T cell hybridomas *in vitro*^{9,10}, but the abilities of these APCs to activate naïve CD8⁺ T cells *in vivo* is uncertain. Others have shown that viruses can induce the synthesis of viral proteins in professional APCs *in vitro* or *in vivo*, but have not linked these observations to antigen presentation *in vivo*^{11,12–14}.

We visualized here the interaction between specific naïve CD8⁺ T cells and virus-infected APCs *in vivo*. These findings directly show that CD8⁺ T cells interact with virus-infected DCs in a local draining lymph node shortly after the introduction of virus into an animal. This interaction is both antigen- and cell type-specific. This conclusion is based on

our failure to observe clustering of CD8⁺ T cells around infected macrophages, despite the fact that infected macrophages outnumbered infected DCs by ~10:1. Substances delivered to PLNs *via* the lymph are unable to access cells in the PLN parenchyma¹⁵; this is unaffected by a concomitant VV infection¹⁵ and strongly suggests that the VV-infected macrophages and DCs we observed in the PLN cortex were infected elsewhere and migrated into the cortex. Given the large numbers of subcapsular macrophages that are infected, it is likely that VV delivered by lymph infects these cells *in situ* and that these cells represent the major source of infected cortex macrophages. DCs, on the other hand, do not typically reside in the subcapsular space. This raises the possibility that they were infected at or near the site of injection and migrated to the PLN *via* the lymphatics. The preferred interaction of CD8⁺ T cells with DCs—as opposed to macrophages—in the cortex could be due to increased expression of costimulatory molecules or increased secretion of chemoattractants and remains to be characterized. We recognize that although we showed that DCs infected *in vitro* were capable of activating CD8⁺ T cells *in vivo* and that CD8⁺ T cells interact with infected DCs *in vivo*, it remains to be formally established that CD8⁺ T cell activation results from this interaction.

There are a number of recent reports that *in vitro* infection of professional APCs with viruses (including VV) interferes with the antigen-presenting functions of these cells^{16,17}. Although these reports postulate that such viruses have evolved to interfere with antigen presentation, such interference is to be expected given the general shutdown in host cell functions that accompany viral infections. Our findings indicate that VV-infected APCs are capable of activating naïve CD8⁺ T cells, probably because presentation of endogenous viral antigens occurs too quickly for the virus-induced alterations in cellular physiology to influence the capacity of APCs to activate CD8⁺ T cells. Direct presentation of VV-encoded antigens is consistent with published data showing that antigens expressed under the control of early VV promoters are more immunogenic than those expressed by late promoters (which actually produced greater amounts of antigen)^{18,19} and that only early viral proteins are produced by VV-infected DCs²⁰.

We not only visualized the interaction of T cells with DCs expressing NP-S-EGFP, we also observed antigen-specific clustering at DCs that did not detectably express the NP-S-EGFP fusion protein. These cells may have been infected, but synthesized the fusion protein in amounts that were insufficient for visualization but sufficient to attract CD8⁺ T cells. Alternatively, these cells may have been cross-presenting NP-S-EGFP acquired from other cells. NP produced by recombinant adenovirus under the control of tissue-specific promoters is capable of priming NP-specific CD8⁺ T cells in a manner that is consistent with cross-priming²¹. The clearest evidence to date to support the occurrence of cross-priming in viral

infections²² was provided when the immunogenicity of OVA produced by a recombinant poliovirus in transgenic mice expressing the poliovirus receptor was analyzed. The experiments showed that although the response required bone marrow-derived APCs, these cells did not need to be infected by poliovirus. Less direct evidence to support the cross-priming of antigen produced in a VV infection *in vivo* has also been reported^{7,23} and, *in vitro*, DCs can cross-present antigen derived from canarypoxvirus-infected cells that are undergoing apoptosis²⁴. VV does not typically induce apoptosis and has gene products that block apoptosis^{25,26}. Nevertheless, it is possible that cross-presentation of antigen from apoptotic (or even necrotic) VV-infected macrophages in the lymph node contributes to the clustering of CD8⁺ T cells around uninfected DCs.

We found that VV-infected APCs are cleared rapidly from the PLNs, even in the absence of transferred CD8⁺ T cells that can accelerate the clearance of infected cells. This resembled the CD4⁺ T cell-mediated clearance of peptide-loaded DCs⁶. However, in the presence of a high frequency of precursors of specific TCR-transgenic CD8⁺ T cells, we found that infected cells were cleared in <24 h, compared to >48 h in the case of CD4⁺ T cells. The extent to which virus-infected cells are cleared by CD8⁺ T cell-mediated lysis *versus* lysis by NK and other immune cells or virus-mediated cell death remains to be established. Given the low numbers of APCs (~3,000 per node), it is conceivable that even low frequencies of precursor virus-specific CD8⁺ T cells could destroy all the APCs. Given the low numbers of APCs (~3,000 per node), it is conceivable that even low frequencies or precursor virus-specific CD8⁺ T cells would be capable of destroying all the APCs. Two findings argue against this, though not conclusively. First, CD8⁺ T cells acquired lytic activity only after infected cells had vanished from the node. Second, infected macrophages were lost despite our failure to observe their contact with CD8⁺ T cells.

Our finding that APCs are rapidly lost from the draining nodes concurs both physically and functionally with reports that brief periods of T cell exposure to antigen-pulsed APCs can lead antigen-specific CD8⁺ T cells to undergo multiple divisions in the absence of further antigen^{27,28}. Together, these observations support a model in which CD8⁺ T cell responses are activated very early in the course of a viral infection by relatively few APCs. This may have evolved to minimize both response times and the potential of viruses to interfere with CD8⁺ T cell activation. Indeed, it is notable that viruses with sophisticated strategies for interfering with CD8⁺ T cell responses (for example, HIV and α - and β -herpesviruses)^{29,30} induce robust CD8⁺ T cell responses³¹. This suggests that these strategies are aimed at blocking the efferent function of CD8⁺ T cells rather than their activation.

Finally, our results suggest that the strong ability of VV to induce CD8⁺ T cells stems in part from its ability to rapidly express large amounts of viral protein in DCs. Notably, foreign proteins expressed in VV are not particularly immunogenic, an effect we have attributed to immunodominance mediated by immunodominant VV-proteins³². Because these proteins are required for VV-infection, it is probably not possible to greatly improve this situation. Rather, the creation of optimal CD8⁺ T cell vaccines will require the development of a vector that, like VV, induces the abundant synthesis of the nominal antigen in PLN DCs and creates the danger signals necessary to induce and maintain CD8⁺ T cell activation^{33,34}, but does so without expressing other foreign proteins.

Methods

Media and cell lines. Media were from Life Technologies (Gaithersburg, MD). The B3Z hybridoma was maintained in RPMI 1640 containing 10% fetal bovine serum (FBS), penicillin, streptomycin, nonessential amino acids, 1 mM sodium pyruvate and 2 mM glutamine (R-10). For cell isolation, primary *ex vivo* cells were suspended in calcium-magnesium-free medium supplemented with 10% FBS.

Mice. TAP1^{-/-} mice³⁵ (from L. Van Kaer, Vanderbilt University School of Medicine) were bred onto a B6 background. OT-I mice³⁶ (from K. Hogquist, University of Minnesota), B6, TAP1^{-/-} and F537 mice were all bred at Taconic Farms (Germantown, NY) under specific pathogen-free conditions.

Viruses. The plasmid pNP-SIINFEKL-EGFP³⁸ consisted of a gene derived from the influenza virus A/Puerto Rico/8/34 fused to chicken OVA(257–264), followed by a COOH-terminal fusion to EGFP from *aequorea victoria* (Clontech, Palo Alto, CA). It was mutated with the Quickchange mutagenesis kit (Stratagene, La Jolla, CA) with the oligonucleotides forward (GCTTCCAATGAAAATATGGATGCTATGGAATCAGTACAC) reverse (GTG TACTTGATTCCATAGCATCCATATTTTCATTGGAAGC). The product of this mutagenesis, pNP366NT60-SIINFEKL-EGFP, has two nucleotide changes; these changes convert an immunodominant determinant of PR8 NP (ASNENMETM) to that of strain A/NT/60/68 (ASNENMDAM). The NP-SIINFEKL-EGFP open-reading frame was removed from pNP366NT60-SIINFEKL-EGFP with *Sall* and *NotI* and cloned into similarly digested pSC11SBAKN. The resulting plasmid, pSC11NP366NT60-SIINFEKL-EGFP, was then used to construct a recombinant vaccinia virus with standard methods³⁹.

Tissue sectioning and microscopy. PLNs were excised at various timepoints after infection, embedded in Tissue Tek OCT (Miles Laboratories, Elkhart, IN), rapidly frozen by immersion in liquid nitrogen-cooled isopentane and kept at -80 °C until use. Cryostat sections (8 μ m and 25 μ m) were cut at -20 °C, mounted on glass slides, air-dried, fixed and processed for immunocytochemistry. Among the various fixatives tested, we found that fixation with 3.2% paraformaldehyde (Electron Microscopy Sciences, Ft. Washington, PA) in 0.15 M PBS, pH 7.4, for 20 min at room temperature give the best results. This was judged by the preservation of EGFP-intrinsic fluorescence, the degree of staining and the quality of the morphology. To avoid nonspecific adherence of antibodies to murine Fc receptors, sections were incubated in Fc Block (BD Pharmingen, San Diego, CA), which contained 10% normal mouse serum (Sigma, St. Louis, MO), for 30 min at room temperature. Then the sections were incubated with the following primary antibodies, which were diluted in this blocking reagent. Red-phycoerythrin (RPE)-conjugated rat anti-mouse I-A^b (clone AF6-120.1), anti-mouse CD3e (clone 145-2C11), anti-mouse CD8 (Ly2, clone 53-6.7), anti-mouse CD45R-B220 (clone RA3-6B2), anti-mouse CD11b (clone M1/70), anti-mouse CD11c (clone HL3) and anti-mouse Ly-6G (clone RB6-8C5) were all from BD Pharmingen. Rat anti-mouse CD169 (sialoadhesin or Siglec-1, MCA884, clone 3d6.112, IgG2a), anti-mouse metallophilic macrophages (clone MOMA1, IgG2a), anti-mouse macrophages-monocytes (MCA519G, clone MOMA2, IgG2b), anti-mouse macrophage scavenger receptor (MCA1322, clone 2f8, IgG2b), anti-mouse dendritic-interdigitating cells (MCA948, clone MIDC-8, IgG2a) and anti-mouse F4/80 (MCA497, clone F4/80, IgG2b) were all from Serotec (Raleigh, NC). The isotype-specific secondary antibodies biotinylated anti-rat IgG2a (RG7/1.30) and anti-rat IgG2b (Rg7/11.1) (PharMingen) followed by Texas red-streptavidin (or Cy5-streptavidin, both from Jackson ImmunoResearch, West Grove, PA) were used to detect the corresponding primary antibodies. Nuclei were stained with TO-PRO-3 iodide (Molecular Probes, Eugene, OR). Sections were mounted in Fluoromount-G (Southern Biotechnology Associates, Birmingham, AL). Staining was visualized with a Zeiss Axioplan fluorescence microscope equipped with an MRC-1024 laser scanning confocal system controlled by Lasersharp 3.2 image acquisition and analysis software from Bio-Rad Laboratories (Hercules, CA). The surface of the cryosection was visualized with a $\times 20$ dry objective. Digital images were aligned and assembled to reconstruct the whole (large) surface area of the sectioned lymph node with Adobe Photoshop 6.0 software (Adobe Systems, Mountain View, CA). The localization of EGFP with various cell markers was analyzed on z-series of high-resolution images (512 \times 512 pixels; 92 nm²/pixel) obtained with a $\times 63$ plan apochromat oil immersion objective and a $\times 2.5$ zoom. In addition, live lymph nodes were visualized with a $\times 40$ water immersion objective. Although we obtained some information using a conventional confocal microscope, most clusters appeared to be deeper than 100 μ m within the node (Fig. 6b). Therefore we also used a multiphoton laser-scanning microscope system Radiance 2000 (BioRad) on an Olympus BX50 upright microscope (Olympus, Melville, NY) (Fig. 6a). Dual photon excitation was obtained from a Ti:Sapphire Millenia pumped Tsunami laser (Spectra Physics, Mountain View, CA) used at 960 nm, with fluorescence emission detected with 515/30 (green) and 600/40 (red) emission filters. Samples were visualized with a $\times 60$ water-immersion objective. A series of images from a 25 μ m-thick volume of the node were recorded over time and processed with Metamorph software (Universal Imaging, West Chester, PA) to obtain Quicktime time-lapse movies.

T cell activation assays. Antigen presentation *ex vivo* was assessed by incubating lymph node cells with the B3Z hybridoma specific for the OVA(257–264)-H-2K^b complex⁵. Lymph nodes were excised, diced and digested in 5 mg/ml of collagenase B (Boehringer, Boehringer-Mannheim, Germany) in calcium-magnesium-free medium containing 10% FCS for 40 min at 37 °C. Approximately 1 \times 10⁶ lymph node cells were incubated with 5 \times 10⁵ B3Z cells overnight, and the percentage of β -galactosidase-positive activated cells scored as described⁴⁰.

To analyze cytolytic activity, lymph nodes were removed and used as effectors in microcytotoxicity assays. Generally, 10⁶ EL4 target cells were labeled with 100 μ Ci of Na²⁴CrO₄ (Amersham, Arlington Heights, IL) in a minimum volume of medium at 37 °C for 60 min. EL4 cells were pulsed with the specific OVA(257–264) peptide or an irrelevant H-K^b-binding peptide, VSV NP(52–59). After two washes, 10⁴ cells were aliquoted into round-bottom, 96-well plates that contained serial dilutions of effector CD8⁺ T cells. The radioactivity in supernatants collected after 4–6 h of incubation at 37 °C was determined using a γ -counter. The percentage specific release was then determined as: % specific release = (CTL-induced release - spontaneous release)/(release by detergent - spontaneous release) \times 100.

To analyze the activation of adoptively transferred TCR-transgenic T cells, spleens were collected ~16 h after infection or immunization, homogenized and centrifuged in prewarmed Ficoll to yield mononuclear cells. Cells were stained with cychrome-anti-CD8 (clone 53-6.7), either anti- $V_{\alpha}2$ (for OT-I, clone B20.1) or anti- $V_{\beta}11$ (for F5, clone RR3-15) and FITC-labeled anti-CD69 (clone H1.2F3), anti-CD25 (clone 7D4) or anti-CD62L (clone 38C-13, all were from BD-Pharmingen). Similar data were obtained with each of the activation markers, with more cells showing up-regulation of CD69 than up-regulation of CD25 or down-regulation of CD62L. This may have reflected the activation of transferred cells in sites that were distinct from the spleen, as injected APCs are likely to be present and able to activate T cells in sites such as the lung and liver after i.v. injection.

Adoptive transfer of T cells. TAP1^{-/-} mice were sublethally irradiated with 800 rads. Lymph nodes (popliteal, inguinal, brachial, axillary and superficial cervical), along with spleens, were removed from F5 OT-I TCR-transgenic mice, homogenized and spun over Ficoll to yield mononuclear cells. A purified T cell population was generated by incubation with anti-CD90 (Thy1.2) beads (Miltenyi Biotech, Auburn, CA) for 15 min on ice; positive cells were then isolated with the AutoMACS system. After this purification, T cell populations were typically 85–95% pure. Between 5×10^6 – 1×10^7 cells were injected into TAP1^{-/-} recipients. Before transfer of F5 or OT-I cells into normal mice, purified T cells were labeled with 10 μ M CMTMR (5-(and-6)-(4-chloromethyl)benzoyl)amino)tetramethylrhodamine (cell tracker orange, Molecular Probes) in medium.

Infection and immunization with primary APCs. For immunization with infected or peptide-pulsed cell populations, spleens were removed from normal B6 mice, cut into small pieces and incubated in collagenase B. The resulting cell population was depleted of red blood cells by incubating in ACK lysis buffer (BioWhittaker, Walkersville, MD) for 5 min, then washed in calcium-magnesium-free medium. Spleen cells were infected with VV at an approximate moiety of infection of 10 for 1 h in balanced salt solution supplemented with 0.1% (w/v) bovine serum albumin washed four times and $\sim 4 \times 10^7$ cells injected into recipient mice. *In vitro* infection of spleen cells infected the majority of cell populations, including macrophages and DCs, but the largest proportion of infected cells were the MHC class II⁺ B cells (data not shown). To deplete infected spleen cells of DCs or B cells, the population was incubated with anti-CD11c or anti-B220 magnetic beads (Miltenyi Biotech), then negatively depleted of the bead-binding population using the AutoMacs system.

Acknowledgments

We thank B. Buschling for excellent technical assistance; M. Princiotto, P. Calvo, P. Berglund, W. Chen and S. Prasad for assistance with animal procedures; B. M. Weinstein (Laboratory of Molecular Genetics, NICHD, NIH) and S. A. Tesfai (Bio-Rad Laboratories) for assistance with multiphoton microscopy experiments; S. Jameson and P. Garside for helpful discussions; and P. Berglund and D. Tschärke for critical review of the manuscript. Supported by the Wellcome Trust (C. C. N.).

Competing interests statement

The authors declare that they have no competing financial interests.

Received 6 September 2001; accepted 8 January 2002.

- Pamer, E. & Cresswell, P. Mechanisms of MHC class I-restricted antigen processing. *Annu. Rev. Immunol.* **16**, 323–358 (1998).
- Rock, K. L. & Goldberg, A. L. Degradation of cell proteins and the generation of MHC class I-presented peptides. *Annu. Rev. Immunol.* **17**, 739–779 (1999).
- Yewdell, J. W., Norbury, C. C. & Bennink, J. R. Mechanisms of exogenous antigen presentation by MHC class I molecules *in vitro* and *in vivo*: implications for generating CD8⁺ T cell responses to infectious agents, tumors, transplants, and vaccines. *Adv. Immunol.* **73**, 1–77 (1999).
- Jenkins, M. K. *et al.* *In vivo* activation of antigen-specific CD4 T cells. *Annu. Rev. Immunol.* **19**, 23–45 (2001).
- Karttunen, J., Sanderson, S. & Shastri, N. Detection of rare antigen-presenting cells by the lacZ-T-cell activation assay suggests an expression cloning strategy for T-cell antigens. *Proc. Natl Acad. Sci. USA* **89**, 6020–6024 (1992).
- Ingulli, E., Mondino, A., Khoruts, A. & Jenkins, M. K. *In vivo* detection of dendritic cell antigen presentation to CD4⁺ T cells. *J. Exp. Med.* **185**, 2133–2141 (1997).
- Norbury, C. C. *et al.* Multiple antigen-specific processing pathways for activating naive CD8⁺ T cells *in vivo*. *J. Immunol.* **166**, 4355–4362 (2001).
- Elliott, T., Willis, A., Cerundolo, V. & Townsend, A. Processing of major histocompatibility class I-restricted antigens in the endoplasmic reticulum. *J. Exp. Med.* **181**, 1481–1491 (1995).
- Hamilton-Easton, A. & Eichelberger, M. Virus-specific antigen presentation by different subsets of cells from lung and mediastinal lymph node tissues of influenza virus-infected mice. *J. Virol.* **69**, 6359–6366 (1995).
- Usherwood, E. J., Hogg, T. L. & Woodland, D. L. Enumeration of antigen-presenting cells in mice infected with Sendai virus. *J. Immunol.* **162**, 3350–3355 (1999).
- MacDonald, G. H. & Johnston, R. E. Role of dendritic cell targeting in Venezuelan equine encephalitis virus pathogenesis. *J. Virol.* **74**, 914–922 (2000).
- Bender, A. *et al.* The distinctive features of influenza virus infection of dendritic cells. *Immunobiology* **198**, 552–567 (1998).
- Ho, L. J. *et al.* Infection of human dendritic cells by dengue virus causes cell maturation and cytokine production. *J. Immunol.* **166**, 1499–1506 (2001).
- Sevilla, N. *et al.* Immunosuppression and resultant viral persistence by specific viral targeting of dendritic cells. *J. Exp. Med.* **192**, 1249–1260 (2000).
- Gretz, J. E., Norbury, C. C., Anderson, A. O., Proudfoot, A. E. & Shaw, S. Lymph-borne chemokines and other low molecular weight molecules reach high endothelial venules via specialized conduits while a functional barrier limits access to the lymphocyte microenvironments in lymph node cortex. *J. Exp. Med.* **192**, 1425–1440 (2000).
- Salio, M., Cella, M., Suter, M. & Lanzavecchia, A. Inhibition of dendritic cell maturation by herpes simplex virus. *Eur. J. Immunol.* **29**, 3245–3253 (1999).
- Engelmayer, J. *et al.* Vaccinia virus inhibits the maturation of human dendritic cells: a novel mechanism of immune evasion. *J. Immunol.* **163**, 6762–6768 (1999).
- Townsend, A. *et al.* Defective presentation to class I-restricted cytotoxic T lymphocytes in vaccinia-infected cells is overcome by enhanced degradation of antigen. *J. Exp. Med.* **168**, 1211–1224 (1988).
- Coupar, B. E. H., Andrew, M. E., Both, G. W. & Boyle, D. B. Temporal regulation of influenza hemagglutinin expression in vaccinia virus recombinants and effects on the immune response. *Eur. J. Immunol.* **16**, 1479–1487 (1986).
- Bronte, V. *et al.* Antigen expression by dendritic cells correlates with the therapeutic effectiveness of a model recombinant poxvirus tumor vaccine. *Proc. Natl Acad. Sci. USA* **94**, 3183–3188 (1997).
- Prasad, S. A., Norbury, C. C., Chen, W., Bennink, J. R. & Yewdell, J. W. Recombinant adenoviruses induce CD8 T cell responses to an inserted protein whose expression is limited to nonimmune cells. *J. Immunol.* **166**, 4809–4812 (2001).
- Sigal, L. J., Crotty, S., Andino, R. & Rock, K. L. Cytotoxic T-cell immunity to virus-infected non-haematopoietic cells requires presentation of exogenous antigen. *Nature* **398**, 77–80 (1999).
- Lenz, L. L., Butz, E. A. & Bevan, M. J. Requirements for bone marrow-derived antigen-presenting cells in priming cytotoxic T cell responses to intracellular pathogens. *J. Exp. Med.* **192**, 1135–1142 (2000).
- Motta, I. *et al.* Cross-presentation by dendritic cells of tumor antigen expressed in apoptotic recombinant canarypox virus-infected dendritic cells. *J. Immunol.* **167**, 1795–1802 (2001).
- Kettle, S. *et al.* Vaccinia virus serpin B13R (SPI-2) inhibits interleukin-1 β -converting enzyme and protects virus-infected cells from TNF- and Fas-mediated apoptosis, but does not prevent IL-1 β -induced fever. *J. Genet. Virol.* **78**, 677–685 (1997).
- Vasilenko, S. T., Meyers, A. F., Vander, H. K. & Barry, M. Vaccinia virus infection disarms the mitochondrion-mediated pathway of the apoptotic cascade by modulating the permeability transition pore. *J. Virol.* **75**, 11437–11448 (2001).
- Kaech, S. M. & Ahmed, R. Memory CD8⁺ T cell differentiation: initial antigen encounter triggers a developmental program in naive cells. *Nature Immunol.* **2**, 415–422 (2001).
- van Stipdonk, M. J., Lemmens, E. E. & Schoenberger, S. P. Naive CTLs require a single brief period of antigenic stimulation for clonal expansion and differentiation. *Nature Immunol.* **2**, 423–429 (2001).
- Tortorella, D., Gewurz, B. E., Furman, M. H., Schust, D. J. & Ploegh, H. L. Viral subversion of the immune system. *Annu. Rev. Immunol.* **18**, 861–926 (2000).
- Yewdell, J. W. & Bennink, J. R. Mechanisms of viral interference with MHC class I antigen processing and presentation. *Annu. Rev. Cell Dev. Biol.* **15**, 579–606 (1999).
- McMichael, A. J. & Rowland-Jones, S. L. Cellular immune responses to HIV. *Nature* **410**, 980–987 (2001).
- Chen, W., Anton, L. C., Bennink, J. R. & Yewdell, J. W. Dissecting the multifactorial causes of immunodominance in class I-restricted T cell responses to viruses. *Immunity* **12**, 83–93 (2000).
- Matzinger, P. Tolerance, danger, and the extended family. *Ann. Rev. Immunol.* **12**, 991–1045 (1994).
- Medzhitov, R. & Janeway, C. A. Jr Innate immunity: impact on the adaptive immune response. *Curr. Opin. Immunol.* **9**, 4–9 (1997).
- Van Kaer, L., Ashton-Rickardt, P. G., Ploegh, H. L. & Tonegawa, S. TAP1 mutant mice are deficient in antigen presentation, surface class I molecules, and CD4⁺ T cells. *Cell* **71**, 1205–1214 (1992).
- Hogquist, K. A. *et al.* T cell receptor antagonist peptides induce positive selection. *Cell* **76**, 17–27 (1994).
- Mamalaki, C. *et al.* Thymic depletion and peripheral activation of class I major histocompatibility complex-restricted T cells by soluble peptide in T-cell receptor transgenic mice. *Proc. Natl Acad. Sci. USA* **89**, 11342–11346 (1992).
- Anton, L. C. *et al.* Intracellular localization of proteasomal degradation of a viral antigen. *J. Cell Biol.* **146**, 113–124 (1999).
- Chakrabarti, S., Brechling, K. & Moss, B. Vaccinia virus expression vector: coexpression of β -galactosidase provides visual screening of recombinant virus plaques. *Mol. Cell Biol.* **5**, 3403–3409 (1985).
- Norbury, C. C., Hewlett, L. J., Prescott, A. R., Shastri, N. & Watts, C. Class I MHC presentation of exogenous soluble antigen via macropinocytosis in bone marrow macrophages. *Immunity* **3**, 783–791 (1995).